A Monitor Unit Verification Calculation in IMRT as a Dosimetry QA

J. H. Kung[1,2], G. T. Y. Chen[1,2], and F. T. Kuchnir[3]

Massachusetts General Hospital, Boston, MA[1], Harvard Medical School, Boston, MA[2], Department of Radiation and Cellular Oncology, The University of Chicago[3]
E-mail: jkung@partners.org

ABSTRACT

In standard teletherapy, a treatment plan is generated with the aid of a treatment planning system, but it is common to perform an independent monitor unit verification calculation (MUVC). In exact analogy, we propose and demonstrate that a simple and accurate MUVC in Intensity Modulated Radiotherapy (IMRT) is possible. We introduce a concept of Modified Clarkson Integration (MCI). In MCI, we exploit the rotational symmetry of scattering to simplify the dose calculation. For dose calculation along a central axis (CAX), we first replace the incident IMRT fluence by an azimuthally averaged fluence. Second, the Clarkson Integration is carried over annular sectors instead of over pie sectors. We wrote a computer code, implementing the MCI technique, in order to perform a MUVC for IMRT purposes. We applied the code to IMRT plans generated by CORVUS. The input to the code consists of CORVUS plan data (e.g., DMLC files, jaw settings, MU for each IMRT field, depth to isocenter for each IMRT field), and the output is dose contribution by individual IMRT field to the isocenter. The code uses measured beam data for Sc, Sp, TPR, $(D/MU)_{ref}$ and includes effects from MLC transmission, and radiation field offset. On a 266 MHZ desktop computer, the code takes less than 15 sec to calculate a dose. The doses calculated with MCI algorithm agreed within +/- 3% with the doses calculated by CORVUS, which uses a 1cm x 1cm pencil beam in dose calculation. In the present version of MCI, skin contour variations and inhomogeneities were neglected.

Key Words: Intensity Modulated Radiotherapy, Monitor Unit Calculation, Dosimetry, Quality Assurance, Hand Calculation

1. INTRODUCTION

The Intensity Modulated Radiotherapy (IMRT) is a new conformal treatment modality which is made possible by advances in Multileaf collimator (MLC) technology, pencil beam modeling [1-3], and inverse treatment optimization algorithms [4-8]. With IMRT, the benefits to a patient are improved dose sparing of normal tissues and a possibility of dose escalation [9-11]. With IMRT, the risk to a patient is from a dose error. There are several potential sources of a dose error: a) inaccuracies in an accelerator and/or MLC controls [12,13], b) patient setup and/or organ motions [14-16], and c) inaccuracy in a dose calculation algorithm. At present, there are three levels of verifying the accuracy of a dose calculation by an IMRT treatment planning system: a) a manufacturer of a commercial treatment planning system, b) a clinic during a commissioning phase of an IMRT system [17-22], c) by patient specific phantom studies. In a patient specific phantom study, an IMRT plan is first generated with a patient CT scan, which contains target volume. The patient optimized fluences are applied to a CT scan of a water equivalent phantom. The essential step involves using the IMRT system to recalculate doses for the phantom geometry. The dosimetry verification is between the measured and the calculated doses for the phantom. A patient specific phantom study is labor intensive. A phantom study also assumes that if D(measured)/D(calculated) for a phantom agrees within a few percent, then D(delivered)/D(calculated) in a patient should also agree within a few percent. This assumption is justified if the phantom and the patient geometries are similar. For sliding window IMRT delivery, a difference in MU settings between phantom and patient plans may complicate the validity of phantom study. One bonus feature of a phantom study is that the study verifies whether an accelerator and/or MLC controls are behaving properly, at least for the day in which the study was performed. In this paper, we propose another patient specific dosimetry quality assurance procedure, i.e., an independent Monitor Unit Verification Calculation in IMRT. The MUVC includes scattered dose, MLC transmission, and a radiation field offset [23-25].

2. METHODS

We begin by making an analogy to a Monitor Unit Verification Calculation (MUVC) in the standard teletherapy. In the standard teletherapy, a treatment plan is generated with the aid of a treatment planning system, but it is a common practice to perform a MUVC. A MUVC requires the following information from a treatment plan: beam energy, accessories (such as wedges), jaw dimensions, equivalent square for a treated area, depth to a point in tissue, and a dose contribution from each field to a chosen point. With this information, we can calculate a required MU for each field. Finally, MU calculated with the MUVC is compared with MU as calculated by a treatment planning system. The MUVC essentially verifies the accuracy of a treatment planning system dose calculating algorithm for a single point in a target volume. In the MUVC, we neglect tissue contour variations and assume a homogeneous water equivalence.

In IMRT, a plan is generated by an IMRT treatment planning system. In exact analogy, one should be able to perform a MUVC in IMRT [Fig. 1]. A MUVC in IMRT should require the following information from a plan: DMLC files, jaw dimensions for collimator scatter factor, MU for each IMRT field (MU/field), depth to isocenter for each IMRT field, and beam energy. Using this information, one should be able to calculate dose contribution by each field (dose/field) to a chosen point in tissue (e.g., isocenter). The sum of dose/field, calculated with MUVC, should agree with dose as calculated by the IMRT system. The details of MUVC in IMRT are explained in each of the following subsections.
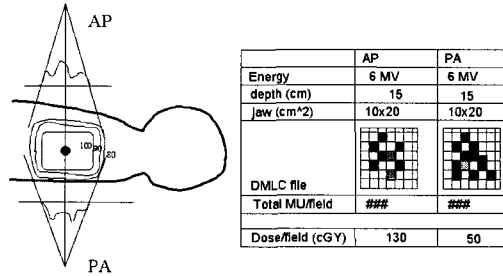

	AP	PA
Energy	6 MV	6 MV
depth (cm)	15	15
jaw (cm^2)	10x20	10x20
DMLC file		
Total MU/field	###	###
Dose/field (cGY)	130	50

Figure 1. A Monitor Unit Verification Calculation (MUVC) in an IMRT.

2.1. Modified Clarkson Integration (MCI) in IMRT

Given a beam energy, jaw dimensions, DMLC file, and MU/field of an IMRT plan, we are interested in some independent method of calculating dose to a point in tissue. A solution to this problem will allow us to perform a MUVC in IMRT. We will first solve the problem of calculating a dose in tissue for points along the central axis (CAX). We will also assume a flat tissue contour and a homogenous tissue. A general case will be addressed in the discussion section. Consider a step and shoot DMLC file, which contains information about MU's and shapes of each static MLC subfield [Fig. 2]. A composite of all MLC subfield openings weighed by MU's of each subfield results in delivered fluence MU(x,y). We include fluence contribution from MLC transmission in the following way. For regions inside the jaws but blocked by MLC, we include (1-2)% of MU of the subfield [26-29] as the transmission fluence. For the Varian round ended MLC with 6MV, the radiation field offset (RFO) is 0.2 mm [23-24]. The RFO is from the penetration of radiation into the rounded leaf heads. $RFO = X(radiation) - X(light)$ at source to axis distance (SAD). X(radiation) and X(light) are radiation and light fields, respectively. In CORVUS, to accommodate for the RFO, all digital positions of leaf openings are made smaller than desired radiation field sizes by the value of RFO. As an example, to generated a radiation field size of ($X_{right}(rad), X_{left}(rad)$) = (10 mm, 10 mm), the digital positions of leaf positions are set to ($X_{right}(light), X_{left}(light)$) = (9.8 mm, 9.8 mm). Therefore, in the reconstruction of delivered fluence from DMLC file, we also used an offset of 0.2 mm. We did not include any second order effects such as tongue and groove; the only MLC head scatter effects used was the Radiation Field Offset.

There is a symmetry in the scattering along the CAX. Fig. 3 shows three 1 cm x 1 cm leaf openings at constant radius R from the CAX, each with identical value of MU. Notice that the three MLC openings contribute equally to a scattered dose along the CAX. Because of the azimuthal symmetry, the problem of converting from a fluence in air to dose in tissue for points along the CAX can be greatly simplified. At each radius, one can replace the MU(x,y) by MU(r), which is an azimuthal average of MU(x,y) at each radius [Fig. 4]

$$MU(x, y) \rightarrow MU(r) \equiv \frac{1}{2\pi} \int_{circle} MU(x, y) d\theta.$$

(1)

As an example [Fig. 5], a dose contribution from an annulus with an inner and an outer radii of $(r, r + \Delta r)$ is just the difference in dose from the disk openings with the radii $r + \Delta r$ and r.

$D(d, \text{annulus}) = D(d, r + \Delta r) - D(d, r)$

$$= \left(\frac{D}{MU}\right)_{ref} (Inv - Sq) S_c MU\left[S_p(r + \Delta r)TPR(r + \Delta r) - S_p(r)TPR(r)\right] \tag{2}$$

Where

$\left(\dfrac{D}{MU}\right)_{ref}$ = Dose per MU at reference depth and field size

S_c = collimator (jaw) scatter factor

S_p = phantom scatter factor

TPR = tissue phantom ratio

$Inv - Sq$ = inverse square factor

$\tag{3}$

In general, a dose is a sum of a primary and the scattered dose [Fig. 6].

$D(d) = D(d, primary) + \sum_{annulus} D(d, annulus)$

$$= \left(\frac{D}{MU}\right)_{ref} (Inv - Sq) S_c\left[MU(0)S_p(0)TPR(0) + \sum_r MU(r)\left[\begin{array}{c} S_p(r + \Delta r)TPR(r + \Delta r) \\ - S_p(r)TPR(r) \end{array}\right]\right] \tag{4}$$

MU(0) represents primary fluence.   In brief, with the Modified Clarkson Integration (MCI), we first perform an azimuthal fluence average along a CAX. Second, the Clarkson integration is over annular sectors instead of over pie sectors [30].
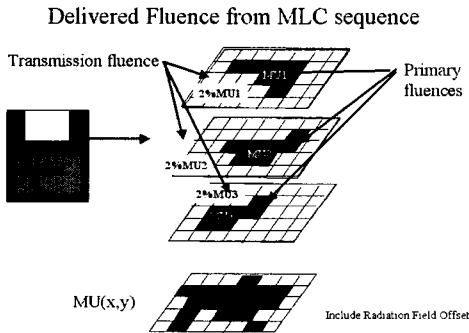

Figure 2.   A calculation of delivered fluence MU(x,y) from a DMLC file.
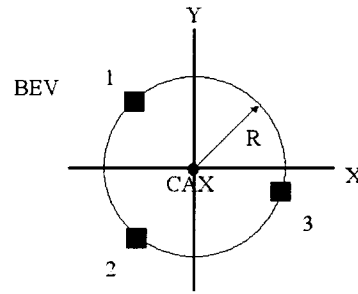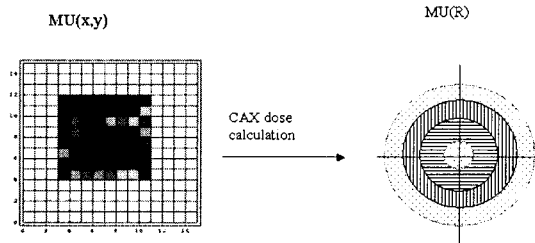

Figure 3.   A scattering symmetry along a central axes (CAX). The three MLC openings contribute equally to a scattered dose along the CAX.

$$MU(x,y) \xrightarrow{\text{replace}} MU(r) \equiv \frac{1}{2\pi} \int_{circle} MU(x,y)d\theta$$

Figure 4.   At each radius, replace MU(x,y) by MU(r), which is an azimuthal average of MU(x,y). The dose along CAX is unchanged.

BEV

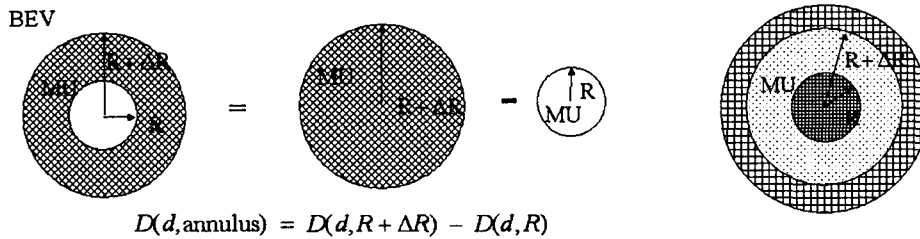$$D(d, \text{annulus}) = D(d, R + \Delta R) - D(d, R)$$

Figure 5. A dose contribution from an annulus with an inner and an outer radii of $(r, r + \Delta r)$ is just the difference in dose from the disk openings with the radii $r + \Delta r$ and r.
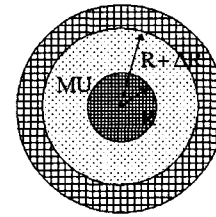

$$D(d) = D(d, \text{primary}) + \sum D(d, \text{annulus})$$

Figure 6. A dose is a sum of primary and scattered doses.

2.2. Computer Code

We wrote a computer code in Mathematica 3.0 (Wolfram Research) to implement the MCI as a MUVC in IMRT. To implement the code, an IMRT plan is first generated with CORVUS (NOMOS Corporation, Sewickley, PA) and the plan information (i.e., DMLC files, jaw settings, MU/field, depth along CAX to isocenter for each IMRT field) is used by the code to calculate dose/field to isocenter. The sum of dose/field was than compared with dose to isocenter as calculated by CORVUS. The delivered fluence MU(x,y) and azimuthal averaged fluence MU(r) are calculated from DMLC files. In the Clarkson Integration, we use saved beam data for Sc, Sp, TPR, MLC transmission factor, RFO, and $(D/MU)_{ref}$. In Sc and Sp, we assumed that a disk of radius r has an equivalent square of 2r x 2r [31]. We used fluence MU(x,y) averaged on a disk of r=1cm for primary fluence MU(0) [32,33]. In the azimuthal fluence averaging, the annuli were concentric circles with a radial increment of $\Delta r = 2 \, mm$. A MLC transmission factor of 2.5% was assumed in both CORVUS and MCI code. Because inhomogeneity correction was not used in CORVUS, for comparison in the MCI code we also used only geometrical depths. On a 266MHZ desktop computer, the code takes less than 15 sec to calculate a dose/field.

3. RESULTS AND DISCUSSION

5 IMRT plans were first generated with the CORVUS using step and shoot IMRT system (Table I). The IMRT plans were for delivery on Varian 2100C with 40 pair Varian MLC. The dose calculation in CORVUS is performed with 1 cm x 1 cm pencil beams, and the optimization is achieved by a simulated annealing technique. Table I shows the comparison of D(MCI) and D(CORVUS). The difference between D(MCI) and D(CORVUS) is +/-3%. During commissioning of CORVUS, we concluded that D(CORVUS) and D(measurement) with ionization chamber were also within +/- 3% for dose calculation along central axis, homogeneous water equivalent phantom, and for points within target volume. We did not perform additional checks to verify the agreement between D(MCI) and D(measurement).

In the code, we used fluence MU(x,y) averaged on a disk of r=1cm for primary fluence MU(0). Therefore D(MCI) per IMRT field is dose as measured by an ionization chamber with an approximate cross section of $\pi r^2 = \pi(1cm)^2$, and the composite of dose/field from all IMRT fields is an average dose to a volume of tissue $\frac{4}{3}\pi r^3 = \frac{4}{3}\pi(1cm)^3$. In order to use MCI as a true point dose calculation engine, the beam data (e.g., Sp and TPR) will have to be extrapolated to the zero field size. The present version of CORVUS does not give information about dose contribution by individual field. Therefore we were not able to compare D(CORVUS) and D(MCI) for each IMRT field.

The present version of the code allows dose calculation only along the central axis (CAX). The code also assumes a flat tissue contour and a homogeneous tissue. In the future, we plan to investigate a general case. For an off axis calculation, the MCI technique should work as long as the azimuthal fluence averaging is performed along an effective CAX [Fig. 7]. For a tissue contour variations [Fig. 8] experience with MUVC in standard teletherapy indicates that depth for a primary beam is the most important. Nevertheless, the MCI can be made to accommodate skin contour variations by using attenuation corrections of incident fluences, such that the calculation can proceed as if the tissue were flat. For an inhomogeneous tissue, all geometrical depths should be replaced with radiological depths. We feel that the MCI is more than an independent "black box" dose calculation engine. Figure 9 shows an example of an azimuthal averaged fluence of an IMRT field. In this example, the profile is approximately 35 MU from R = 0 cm to R = 4 cm and the profile drops sharply for radius larger than 4 cm. Therefore a simple hand calculation can be used.

Table 1. Testing the MCI algorithm for MUVC in IMRT. 5 IMRT plans were generated with CORVUS system. The IMRT plan informations were used as inputs into MCI code to generate independent calculations of dose/field to an isocenter.

Site	Comment	# of fields	Dose Point	D(MCI)/D(CORVUS)
Pancreas	Patient CT	9 fids	isocenter	99%
Pancreas boost	Patient CT	9 fids	isocenter	101%
Pituitary	Patient CT	9 fids	isocenter	97%
U shaped target	Cylinder phantom*	7 fids	isocenter	102%
Convex target	Cylinder phantom*	5 fids	isocenter	103%

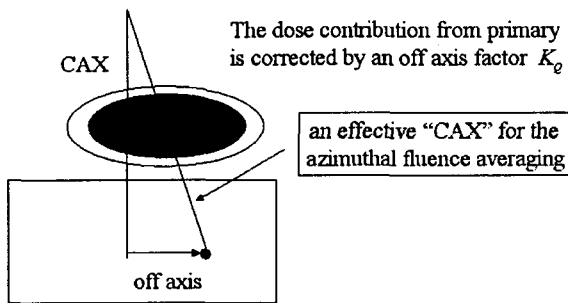* Cylinder was a 8.8cm diameter Lucite phantom

Figure 7. In MCI for an off axes dose calculation, azimuthal fluence averaging is along an effective CAX. There is an additional correction for an off axes factor.
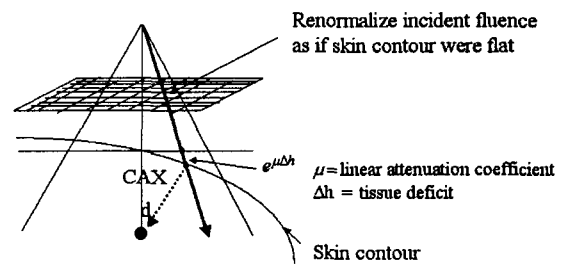
Figure 8. In MCI with tissue contour variations, incident fluence is attenuation corrected for any tissue deficit. After rescaling of incident fluence, all calculation can proceed as if the tissue were flat.
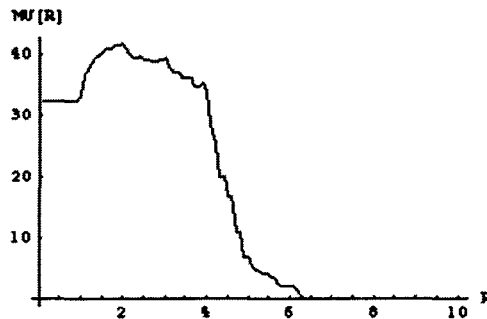

Figure 9. A example of an azimuthally averaged fluence profile MU(r) that allows for a simple hand calculation of dose.

Acknowledgement

REFERENCES

1. J.D. Bourland, E. L. Chaney, "A Finite Size Pencil Beam Model for Photon Dose Calculations in Three Dimensions," Med. Phys. 19, 1401-1412 (1992).
2. T. R. Mackie, J. W. Scrimger, J. J. Battista, "A Convolution Method of Calculating Dose for 15MV X Rays," Med. Phys. 12, 188-196 (1985).
3. A. L. Boyer, E.C. Mok, "A Photon Dose Distribution Model Employing Convolution Calculation," Med. Phys. 12, 169-177 (1985).
4. S. Webb, "Optimization of Conformal Radiotherapy Dose Distributions by Simulated Annealing," Phys. Med. Biol. 34, 1349-1379 (1990).
5. S. M. Morrill, R. G. Lane, G. Jacobson, I. Rosen, "Treatment Planning Optimization Using Constrained Simulated Annealing," Phys. Med. Biol. 36, 1341-1361 (1991).

6. T. Bortfeld, "Methods of Image Reconstruction from Projections Applied to Conformation Therapy," Phys Med. Biol. **35**, 1423-1434 (1990).

7. R. Mohan, X. Wang, A. Jackson, T. Bortfeld, et al., "The Potential and Limitations of the Inverse Radiotherapy Technique," Radiother. Oncol. **32**, 232-248 (1994).

8. L. Xing, G. T. Y. Chen, "Iterative Methods for Inverse Treatment Planning," Phys. Med. Biol. **41**, 2107-2123 (1996).

9. S. A. Leibel, M. J. Zelefsky, G. J. Kutcher, et al., "Three Dimensional Conformal Radiation Therapy at the Memorial Sloan Ketttering Cancer Center," Semin. Radiat. Oncol. **2**, 274-290 (1992).

10. S. Vijayakumar, T. Y. Chen, "Implementation of Three Dimensional Conformal Radiation Therapy: Prospects, Opportunities, and Challenges," Int. J. Radiat. Oncol. Biol. Phys. **33**, 979-983 (1995).

11. D. E. Wazer, N. M. Ling, B. Kramer, et al., "Approaches to Clinical Applications of Intensity Modulated Radiation Therapy for Malignant Tumor of the CNS," In: Sternick, E. S., ed. The Theory and Practice of Intensity Modulated Radiotherapy. Madison, WI: Advanced Medical Publishing; 1996.

12. C. S. Chui, S. Spirou, T. LoSasso, "Testing of dynamic multileaf collimation," Med. Phys. **23**, 635-641 (1996).

13. P. J. Biggs, "Evidence for a Significant Timer Error on a Linear Accelerator: Consequence for a Special Therapy Application," Phys. Med. Biol. **10**, 3139-3143 (1998).

14. C. X. Yu, D. A. Jaffray, J. W. Wong, "The Effects of Intra Fraction Organ Motion on the Delivery of Dynamic Intensity Modulation," Phys. Med. Biol. **43**, 91-104 (1998).

15. J. S. Tsai, M. J. Engler, M. N. Ling, et al., "A Non-Invasive Immobilization System and Related Quality Assurance for Dynamic Intensity Modulated Radiation Therapy of Intracranial and Head and Neck Disease," Int. J. Radiat. Oncol. Biol. Phys. **43**, 455-467 (1999).

16. J. Lof, B. K. Lind, A. Brahme, "An Adaptive Control Algorithm for Optimization of Intensity Modulated Radiotherapy Considering Uncertainties in Beam Profiles, Patient Set-up and Internal Organ Motion," Phys. Med. Biol. **43**, 1605-1628 (1998).

17. A. Wu, M Johnson, A. S. Chen, S. Kalnicki, "Evaluation of Dose Calculation Algorithm of the Peacock System for Multileaf Intensity Modulation Collimator," Int. J. Radiat. Oncol. Biol. Phys. **36**, 1225-1231 (1996).

18. D. A. Low, S. Mutic, "A Commercial IMRT Treatment Planning Dose-Calculation Algorithm," Int. J. Radiat. Oncol. Biol. Phys. **41**, 933-937 (1998).

19. J. S. Tsai, D. E. Wazer, M. N. Ling, et al., "Dosimetric Verification of the Dynamic Intensity Modulated Radiation Therapy of 92 Patients," Int. J. Radiat. Oncol. Biol. Phys. **40**, 1213-1230 (1998).

20. K. Preiser, T. Bortfeld, K. Hartwig, et al., "Inverse Radiotherapy Planning for Intensity Modulated Photon Fields. Radiologe," **38**, 228-234 (1998).

21. A. Boyer, L. Xing, C. M. Ma, B. Curran, et al., "Theoretical Considerations of Monitor Unit Calculations for Intensity Modulated Beam Treatment Planning," Med. Phys. **26**, 187-195 (1999).

22. L. Xing, B. Curran, R. Hill, T. Holmes, et al," Dosimetric Verification of a Commercial Inverse Treatment Planning System," Phys. Med. Biol. **44**, 463-478 (1999).

23. T. LoSasso, C. S. Chui, C. C. Ling, "Physical and dosimetric aspects of a multileaf collimation system used in the dynamic mode for implementing intensity modulated radiotherapy," Med. Phys. **25**, 1919-1927 (1998).

24. A. L. Boyer, S. Li, "Geometrical analysis of light-field position of a multileaf collimator with curved ends," Med. Phys. **24**, 757-762 (1997).

25. J. H. Kung, G. T. Y. Chen, "IMRT Dose Delivery Error from Radiation Field Offset (RFO) Inaccuracy," Submitted to Medical Physics.

26. J. M. Galvin, A. R. Smith, B. Lally, "Characterization of multi-leaf collimator system," Int. J. Radiat. Oncol. Biol, Phys. **25**, 181-192 (1993).

27. C. S. Chui, T. LoSasso, S. Spirou, "Dose calculations for photon beams with intensity modulation generated by dynamic jaw or multi-leaf collimation," Med. Phys. **21**, 1237-1243 (1994).

28. C. S. Chui, R. Mohan, "Algorithms for dynamic jaws and multileaf collimators, II-Fluence distribution," Med. Phys. **20**, 885 (1993) (abstr).

29. J. M. Galvin, A. R. Smith, R. D. Moeller, et. al., "Evaluation of multi-leaf collimator design for a photon beam," Int. J. Radiat. Oncol. Biol. Phys. **23**, 789-801 (1992).

30. J. R. Clarkson, "A Note on Depth Doses in fields of Irregular Shape," Brit. J. Radiol. **14**, 265 (1941).

31. B. E. Bjarngard, R. L. Siddon, "A Note on Equivalent Circle, Squares, and Rectangles," Med. Phys. **9**, 258-260 (1992).

32. B. E. Bjarngard, P. Petti, "Description of the Scatter Components in Photon Beam Data," Phys. Med. Biol. **33**, 1-32 (1988).

33. P. Nizin, G. X. Qian, H. Rashid, "Zero Field Dose Data for Co(60) and Other High Energy Photon in Water," Med. Phys. **20**, 1353-1360 (1993).